Catalysis Science & Technology

PAPER

View Article Online
View Journal | View Issue

Open Access Article. Published on 29 February 2016. Downloaded on 2/9/2026 11:39:55 PM.
This article is licensed under a Creative Commons Attribution-NonCommercial 3.0 Unported Licence.

Cite this: *Catal. Sci. Technol.*, 2016, **6**, 4970

Kinetic studies of fluorinated aryl molybdenum(II) tricarbonyl precursors in epoxidation catalysis†

Robert M. Reich,[a] Marlene Kaposi,[a] Alexander Pöthig[b] and Fritz E. Kühn*[a]

Received 20th December 2015,
Accepted 28th February 2016

DOI: 10.1039/c5cy02220g

www.rsc.org/catalysis

Benzyl substituted molybdenum tricarbonyl complexes displaying CF_3 groups are synthesized and applied as catalyst precursors in olefin epoxidation reactions. The CF_3 moiety is important for both decarboxylation velocity and active species formation. DFT calculations as well as ^{1}H, ^{13}C, ^{19}F and ^{95}Mo NMR spectroscopy help explain the observed reactivity differences. A variety of olefins can be epoxidized and TOFs of up to *ca.* 22 000 h^{-1} are obtained in hexafluoroisopropanol (HFIP). Furthermore, it is possible to recycle the active species at least 10 times without significant activity loss in a two-phase catalytic reaction. ^{19}F NMR kinetic studies reveal that at least two intermediates are formed during the reaction with excess TBHP, depending on the position of the CF_3 group. The substrate addition mode has also a major influence on the catalyst formation velocity.

Introduction

Epoxides are important starting materials or intermediates for a broad variety of chemical products including cosmetics, pharmaceuticals or polymers.[1–3] Oxidations of ethylene and propylene are important large-scale industrial processes as their products are important building blocks for polymers.[1,2,4] A state of the art process for the oxidation of these rather simple olefins is the use of heterogeneous silver (on alumina) catalysts or gold-doped titanium-based catalysts with oxygen or hydrogen peroxide as oxidants.[2–4] However, these heterogeneous systems are not well suited for higher or more sophisticated olefin synthesis, due to harsh reaction conditions, low selectivity and other problems.[2,4]

Homogeneous catalysis may help circumvent some of the disadvantages encountered in heterogeneous systems. A prominent example of catalytic epoxidation is the Halcon–ARCO process (industrially established in the 1960s) which uses $[Mo(CO)_6]$ as a pre-catalyst.[2,5] In order to better understand and improve this process, a variety of molybdenum-based catalyst precursors have been synthesized over the past decades.[6–11] Some of them rival or surpass the well-examined (but unfortunately quite expensive) methyltrioxorhenium (MTO) in terms of catalytic activity.[12,13] MTO was originally established as an epoxidation catalyst by Herrmann *et al.* in 1991.[14] In contrast to MTO where extensive work has provided a commonly accepted mechanism,[14,15] mechanisms of molybdenum-based epoxidation reactions are still disputed. This is not surprising, however, since the structural variety of compounds applicable in epoxidation catalysis is far greater than in the case of Re. Nevertheless, in the 1970s, a generalization of epoxidation mechanisms has been attempted, producing two rather different mechanistic proposals by Mimoun[16,17] and Sharpless *et al.*[18] A multi-step mechanism including olefin pre-coordination to a metal centre, followed by olefin insertion into a metal–peroxo bond was proposed by Mimoun *et al.* A five-membered metallacycle has been assumed to act as an intermediate. Sharpless suggested that an olefin reacts directly with one of the peroxide oxygen atoms, forming a spiro-like transition state. Many mechanistic studies followed to prove or disprove these original proposals. Thiel *et al.*, for example, presented a study using TBHP as an oxidant for molybdenum precursors and obtained results largely in accord with Sharpless' proposal.[19] Some later DFT studies focusing on molybdenum cyclopentadienyl tricarbonyl complexes as catalyst precursors[20–24] showed that the energy barriers for possible intermediates during catalysis are too similar to be distinguished without further experimental evidence. Recently, fluorinated moieties were attached to molybdenum tricarbonyl complexes to get additional mechanistic evidence (*via* ^{19}F NMR spectroscopy) and to reach potentially higher activities due to enhanced Lewis activity *via* a more electron deficient Mo atom.[25,26]

In continuation of our previous examinations of related systems,[25–27] we utilized arylated molybdenum tricarbonyl

[a] *Molecular Catalysis, Department of Chemistry and Catalysis Research Center, Technische Universität München, Lichtenbergstr. 4, D-85747 Garching bei München, Germany. E-mail: fritz.kuehn@ch.tum.de; Fax: +49 89 289 13473; Tel: +49 89 289 13096*

[b] *Catalysis Research Center, Technische Universität München, Ernst Otto Fischer-Str. 1, D-85747 Garching bei München, Germany*

† Electronic supplementary information (ESI) available. CCDC 1441618–1441621. For ESI and crystallographic data in CIF or other electronic format see DOI: 10.1039/c5cy02220g

This journal is © The Royal Society of Chemistry 2016

Open Access Article. Published on 29 February 2016. Downloaded on 2/9/2026 11:39:55 PM.
This article is licensed under a Creative Commons Attribution-NonCommercial 3.0 Unported Licence.

complexes and modified them by varying the position and number of CF_3 group(s) on a benzyl moiety attached to a $CpMo(CO)_3$ entity. The resulting compounds were applied in epoxidation catalysis.

Results and discussion

Synthesis and characterization

The reaction of $Na[CpMo(CO)_3]$ with fluorinated arylbromides leads to air and moisture stable compounds **1–4** in yields of 90–95% under ambient conditions (Scheme 1).

Formation of the compounds is confirmed by ^{1}H, ^{13}C, ^{19}F NMR spectroscopy, IR spectroscopy, elemental analysis and X-ray crystallography (Fig. 1). When compared to literature-known benzylated and pentafluorobenzylated derivatives, the structures of the four compounds are most similar to a pentafluorobenzylated compound with respect to the observed bond angles.[27]

As the infrared spectra of complexes of the type $[CpMo(CO)_3R]$ are well understood, this method was also applied here (see Table 1).[28–31] However, the mean stretching frequencies are very similar for compounds **1–4**. Therefore, ^{95}Mo NMR spectroscopy was utilized in order to find variations caused by the ligand substitution pattern. Downfield shifts are indicative of an increased Lewis acidity at a metal centre in the case of structurally closely related compounds.[12,20,27,32]

The ^{95}Mo NMR peak of compound **1** is the most low field shifted among the examined compounds. This is in accord with the calculated Lewis acidity of the metal centre (see the ESI† S4). It is interesting to note that one additional CF_3 group in the *meta* position in **4** also leads to a distinct low field shift (compared to that in **2**).

Tricarbonyl molybdenum complexes are usually used as precursors in oxidation catalysis since they are relatively easy to handle as they are quite air and moisture stable. A drawback is that induction periods can arise during catalysis due to the (slow) decarbonylation process prior to the formation of active species. This was observed, for example, when comparing $[CpMo(CO)_3CH_3]$ and its trifluorinated derivative. Fluorination leads to prolongation of the decarbonylation process in that case.[26] However, the (oxidized) trifluoromethyl Mo(VI) compound is much more active in oxidation catalysis than its methyl derivative, presumably due to its enhanced Lewis acidity. Recently, we were able to demonstrate that insertion of a CH_2 bridge in arylated fluorinated and non-fluorinated molybdenum tricarbonyl complexes helps ease the decarbonylation process.[27]

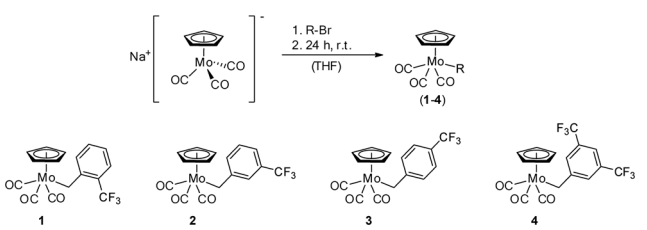

Scheme 1 Synthesis and structure of the organomolybdenum tricarbonyl complexes **1–4**.

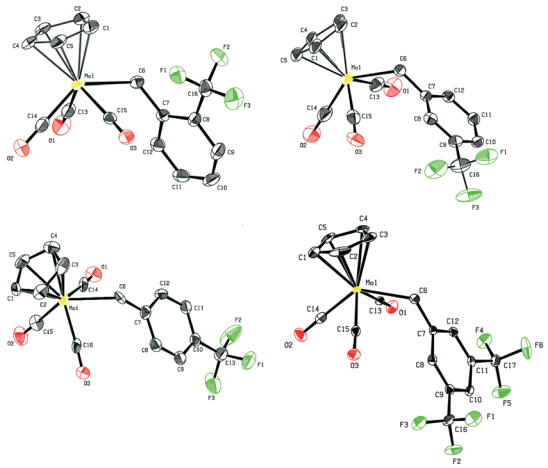

Fig. 1 ORTEP-style presentation of the molecular structures of compounds **1** (upper left), **2** (upper right), **3** (lower left) and **4** (lower right). Ellipsoids are shown at a 50% probability level. Hydrogen atoms are omitted for clarity (carbon: black, oxygen: red, fluorine: green, molybdenum: yellow). For detailed information, see the ESI† S1.

A further systematic account on the influence of fluorination on the catalytic epoxidation activity of Mo compounds is given below, based on varying the number and position of CF_3 groups on a benzyl moiety.

Influence of the position of a CF_3 group on catalysis

To determine the influence of the position of CF_3 on catalytic performance, kinetic studies with the benchmark substrate *cis*-cyclooctene using *tert*-butylhydroperoxide (TBHP) as oxidant have been carried out. The solvent of choice for mechanistic purposes is $CHCl_3$ as it was recently found that decarbonylation is quite slow in it and is therefore easier to follow and to distinguish from the catalytic epoxidation process.[20,27] Unfortunately, as the oxidized derivatives and the active species could not be isolated a – at least at first glance – somewhat clumsy pathway to unravel more mechanistic details is necessary. Comparison of the behaviour of **1–3** shows an increasing induction period (which occurs under applied conditions only with a low excess of TBHP) with an increasing distance from the metal centre to the CF_3 moiety (Fig. 2).

Influence of an additional CF_3 group on catalysis

If a second CF_3 group is present (compound **4**) the catalytic activity is higher (TOF: 2.8 h^{-1}), compared to those of compounds **1** (TOF: 1.2 h^{-1}) and **2** (TOF: 2.4 h^{-1}) (Fig. 2).

Compound **4** is additionally compared to known pentafluorobenzylated and benzylated molybdenum tricarbonyl complexes.[27] Compound **4** has a similar activity to $[CpMo(CO)_3BzF_5]$ (TOF: 2.9 h^{-1}). This shows that the addition of two CF_3 groups to the benzyl moiety has a similar effect to full fluorination of the benzyl ring (Fig. 3).

Open Access Article. Published on 29 February 2016. Downloaded on 2/9/2026 11:39:55 PM.
This article is licensed under a Creative Commons Attribution-NonCommercial 3.0 Unported Licence.

Table 1 Stretching frequencies [cm^{-1}] and ^{95}Mo NMR shifts [ppm] of compounds **1–4**

Stretching frequencies [cm^{-1}]	1	2	3	4
CO sym. stretch	2008.9	2005.9	2008.1	2014.8
CO asym. stretch	1986.1	1970.3	1972.5	1950.6
CO asym. stretch	1911.4	1900.0	1902.7	1916.3
Mean of summarised stretching frequencies [cm^{-1}]	1968.8	1958.7	1961.1	1960.1
^{95}Mo NMR shifts [ppm]	−1525.24	−1558.49	−1562.52	−1537.10

(for details, see the ESI S3).

For the sake of comparison, compound **4** is also compared to [$CpMo(CO)_3Cl$] (TOF: 1.7 h^{-1}) and methyltrioxorhenium (MTO; TOF: 4.0 h^{-1}) as benchmark pre-catalysts in homogeneous oxidation catalysis (Fig. 4).[14,26,33–35]

However, it has to be mentioned that a comparison under these conditions has to be taken with great care, especially since MTO is (considerably) more reactive with hydrogen peroxide as an oxidant. The pre-catalyst to substrate/oxidant ratio was chosen to primarily determine the induction periods. Therefore, a comparison of turnover frequencies under optimised conditions is more useful as it leads to a more realistic appraisal of the compounds as pre-catalysts in oxidation catalysis.

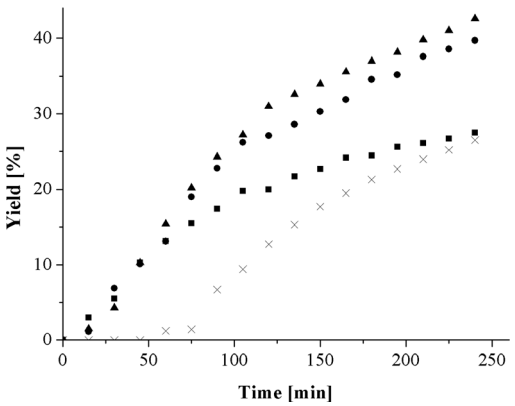

Fig. 2 Kinetic curves of **1** (■), **2** (●), **3** (X) and **4** (▲). Pre-catalyst: *cis*-cyclooctene : TBHP ratio = 1 : 10 : 20 in 0.5 ml of $CDCl_3$, internal standard: mesitylene, T = RT, epoxide selectivity: 99% (yield and selectivity were determined *via* ^1H NMR spectroscopy).

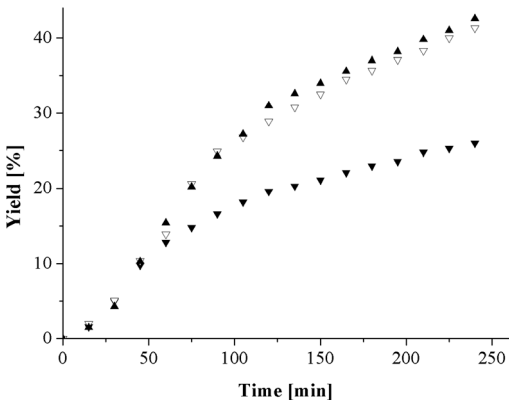

Fig. 3 Kinetic curves of **4** (▲), [$CpMo(CO)_3BzF_5$] (▽) and [$CpMo(CO)_3Bz$] (▼). Pre-catalyst: *cis*-cyclooctene : TBHP ratio = 1 : 10 : 20 in 0.5 ml of $CDCl_3$, internal standard: mesitylene, T = RT, epoxide selectivity: 99% (yield and selectivity were determined *via* ^1H NMR spectroscopy).

Turnover frequencies, substrates and recycling

The application of benzene and hexafluorobenzene (HFB) as solvents to reach high TOFs has been reported previously.[27] In this study, hexafluoroisopropanol (HFIP) has been utilized additionally, as a previous research study shows that it is able to distinctly enhance the velocity of decarbonylation (Table 2).[25] The obtained epoxidation activity correlates well with the Lewis acidity of the compounds (**1** > **4** > **2** > **3**) derived from ^{95}Mo NMR spectroscopy and DFT calculations (see Table 1 and ESI† S4.5). Although the differences are not very pronounced, *i.e.* in the same order of magnitude, it is interesting to note that the position of the CF_3 group on the aromatic ring seems to have a similar impact to an additional CF_3 group. The reason is probably that the *ortho* CF_3 group is located close to the metal centre,

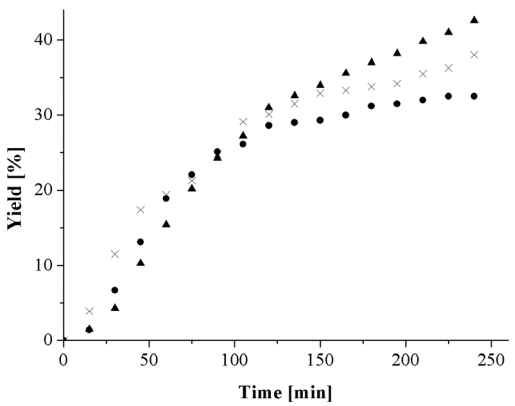

Fig. 4 Kinetic curves of **4** (▲), MTO (X) and [$CpMo(CO)_3Cl$] (●). Pre-catalyst: *cis*-cyclooctene : TBHP ratio = 1 : 10 : 20 in 0.5 ml of $CDCl_3$, internal standard: mesitylene, T = RT, epoxide selectivity: 99% (yield and selectivity were determined *via* ^1H NMR spectroscopy).

Table 2 Turnover frequencies for **1–4** with different solvents[a]

Entry	Solvent	TOFs [h^{-1}] 1	2	3	4
1	Benzene	15 100	12 700	12 000	14 900
2	HFB	18 400	15 300	14 800	18 300
3	HFIP	22 600	19 100	18 500	22 200

[a] Pre-catalyst: *cis*-cyclooctene : TBHP ratio (0.05 : 100 : 200) in 0.5 ml of solvent, internal standard: mesitylene, T = 55 °C, after 5 min. Determination *via* ^1H NMR spectroscopy.

 This journal is © The Royal Society of Chemistry 2016

Open Access Article. Published on 29 February 2016. Downloaded on 2/9/2026 11:39:55 PM.
This article is licensed under a Creative Commons Attribution-NonCommercial 3.0 Unported Licence.

leading to the observed enhanced Lewis acidity and activity in catalysis, whereas the CF_3 groups at the *meta* position are too far away from the centre and exercise no mesomeric effect on the α-carbon atom of the ring.

Using HFIP as solvent, TOFs of over 22 000 h^{-1} can be obtained for compounds **1** and **4**, outperforming fluorinated compounds reported previously under the same conditions (Fig. 5).[25,27]

Compounds **2** and **4** were then chosen to oxidize more sophisticated substrates to evaluate the influence of an additional CF_3 group on catalysis (Table 3). In all the cases, compound **4** is more active than **2**, showing that the additional CF_3 group enhances – as already expected and observed for *cis*-cyclooctene – the overall catalytic activity. For *cis*-stilbene, **4** has a distinct positive influence on the activity compared to **2**, outperforming some previously studied pre-catalysts.[27,36]

Although the TOF shows that this compound is only about half as active (with TBHP as the oxidant) as MTO (with H_2O_2 as the oxidant) (40 000 h^{-1}),[37] it has one substantial advantage. It is possible to recycle the active species of compound **4** for at least 10 successive runs without significant loss in activity in a two-phase reaction with the RTIL (room temperature ionic liquid) $[C_1C_1C_8im][NTf_2]$ as solvent (Fig. 6).

An even roughly similar recycling procedure has not been reported for MTO so far. Further tuning of these molybdenum-based complexes and epoxidation conditions might also lead to a distinct increase in activity, possibly allowing to come closer to a very well optimized MTO system.

Mechanistic studies – ^1H, ^{13}C, ^{19}F and ^{95}Mo NMR spectroscopy

Several computational and experimental studies concerning the general mechanism of epoxidation catalysis with molybdenum tricarbonyl complexes and the formation of certain species, which might also act as pre-catalysts, were performed by the groups of Poli,[23] Calhorda[24] and our group.[20–22]

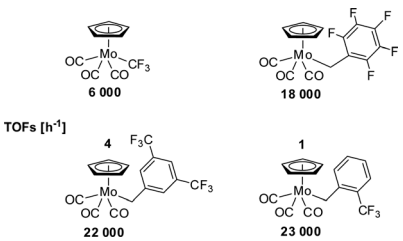

Fig. 5 Comparison: TOFs of $[CpMo(CO)_3CF_3]$, $[CpMo(CO)_3BzF_5]$, **1** and **4**.

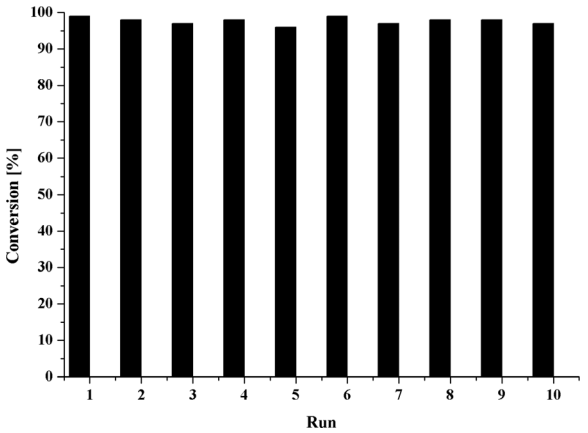

Fig. 6 Recycling experiments using compound **4**. Pre-catalyst : *cis*-cyclooctene : TBHP ratio = 0.5 : 100 : 200 in 0.5 ml of benzene, internal standard: mesitylene, T = 55 °C, after 24 h. Determination *via* ^1H NMR spectroscopy (selectivity: 99%).

These examinations indicate that at least two species are formed as intermediates in the course of the reaction: a dioxo species and an oxo–peroxo species. These species, however, are apparently not the active species as they are unable to transfer an oxygen atom to an olefin without the presence of an additional oxidant. Further species formed during the epoxidation process have been noted.[20]

^1H, ^{13}C, ^{19}F and ^{95}Mo NMR spectroscopic examinations have been applied to check the formation of more intermediates. Especially, ^{19}F NMR spectroscopy (which is possible due to the CF_3 group) seems to be a sensitive tool giving helpful hints on possible intermediates and the velocity of decarbonylation. The kinetic plots during the reaction with excess TBHP in ^{19}F NMR spectroscopy are shown in Fig. 7. It can be seen that at least two species (for **1** and **3**) are formed. For compound **4**, four species are observable. The formation of a light bluish insoluble species **I** (see the Experimental section for the elemental analysis and mass spectroscopy), as already noted before during catalysis,[20] occurs as well. In previous studies, it was not clear, however, if an organic entity R is present in this precipitate. As fluorine is present (in this case) in

Table 3 Substrate scope of **2** and **4**[a]

		2		4	
Entry	Substrate	Conv. [%]	Sel. [%]	Conv. [%]	Sel. [%]
1	*cis*-Cyclooctene	100	99	100	99
2	1-Hexene	75	40	82	78
3	1-Octene	44	99	56	99
4	1-Decene	38	99	49	97
5	*cis*-Stilbene	64	99	78	99
6	*trans*-β-Methylstyrene	32	56	74	70

[a] Pre-catalyst : olefin : TBHP ratio (1 : 100 : 200) in 0.5 ml of C_6D_6, internal standard: mesitylene, T = 55 °C, after 24 h (Conv.: conversion and Sel.: selectivity were determined *via* ^1H NMR spectroscopy).

Open Access Article. Published on 29 February 2016. Downloaded on 2/9/2026 11:39:55 PM.
This article is licensed under a Creative Commons Attribution-NonCommercial 3.0 Unported Licence.

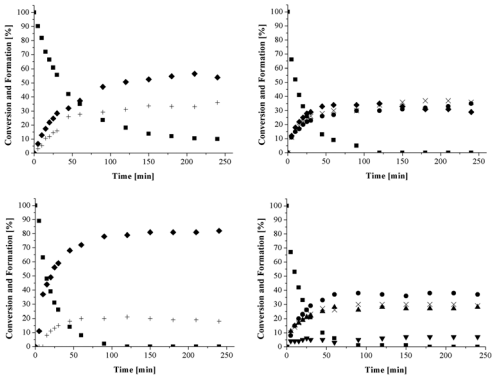

Fig. 7 Kinetic plots of 1 mmol of compounds **1** (upper left), **2** (upper right), **3** (lower left) and **4** (lower right) with 20 eq. of TBHP, T = 55 °C. ■: CF_3 shift of the tricarbonyl precursor. Other symbols: observed CF_3 shifts which form during the reaction with the oxidant. The reaction was monitored by ^{19}F NMR spectroscopy in 0.5 ml of C_6D_6 using HFB as the internal standard.

the elemental analysis (which is part of the ligand R), it can be now concluded that the ligand is part of the insoluble species. Nevertheless, further research is necessary to obtain better insights into the true nature of the precipitate. Interestingly, it appears that the catalytic activity of the compounds correlates with the formation of the insoluble species Table 4.

Further mechanistic investigations were carried out using compound **2**. Three different Cp signals are also observed in the ^1H NMR spectra during the reaction with 20 eq. of TBHP (T = 55 °C) at 4.94, 4.74 and 4.52 ppm (tricarbonyl precursor: 4.69 ppm; for details, see the ESI† Fig. S2.5). The methylene bridge also shifts (in the precursor found at 2.80 ppm) and new downfield shifts appear at 3.49 and 3.31 ppm. Additionally, new peaks at 6.14 ppm appear, which cannot be assigned to an oxo–peroxo or dioxo species and might therefore be an intermediate, as predicted by calculations (see the ESI† Fig. S2.5).[20]

^{13}C NMR spectroscopy provides additional details: first, it shows that the decarbonylation observed in ^{19}F NMR spectroscopy correlates with the decrease in carbonyl signals (for details, see the ESI† Fig. S2.6). Additionally, downfield shifts of aryl carbons are observed (at 160.49 and 173.74 ppm; for details, see the ESI† Fig. S2.7), indicating the formation of new species, presumably dioxo and oxo–peroxo species, as reported before (changes of the shifts are due to the nonpolar solvent C_6D_6 used in this study in comparison to previous studies performed in $CDCl_3$).[20] Additionally, the carbon of the methylene bridge is shifted downfield from 4.62 ppm (precursor) to 31.75 ppm lying in the range expected for a high oxidation state oxo–peroxo species. The methylene bridge of the dioxo species cannot be observed, possibly due to the low concentration and the fast oxo–peroxo species formation reaction.

Also, two new cyclopentadienyl (Cp) signals (precursor with a shift at 95.35 ppm in C_6D_6) at 81.02 ppm and 69.92 ppm are observed, which may be attributed to oxo–peroxo and dioxo species (see Fig. 8). A closer look shows that there are several more Cp signals, which might be the reason for the observation of a third species in the ^{19}F NMR spectra (see the ESI† Fig. S2.8). However, it appears reasonable to assume that the oxo–peroxo and dioxo species are the main species formed in the catalytic oxidation of compound 2 with TBHP.

As previously reported, the presence of both a substrate and an oxidant has a great influence on the formation of different active species.[20] As ^{19}F NMR spectroscopy has been proven to be a sensitive tool in the investigation of different intermediates in the reaction of a pre-catalyst with an oxidant, it was also chosen as a suitable method for examining the reaction of the carbonyl catalyst precursors with an oxidant and a *cis*-cyclooctene substrate (Fig. 9). It shows that slower decarbonylation of the pre-catalyst is apparent in the presence of both a substrate and an oxidant (most likely due to the competition for oxidation) and that one intermediate is favoured (in contrast to the reaction without a substrate – see Fig. 8, upper right). Slower decarbonylation is both evident in ^{13}C (remaining Cp signal of the precursor after 240 min) and ^{95}Mo NMR spectroscopy (see the ESI† Fig. S2.9 and S2.10).

Additionally, 5% of the by-product (the insoluble light blue species) is formed (20% without a substrate). However, it has to be mentioned that the ^{13}C NMR spectra hints at only two main species. A possible explanation for the differences

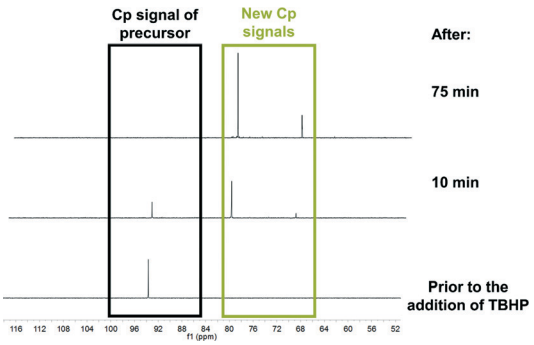

Fig. 8 ^{13}C NMR kinetics show the formation of two cyclopentadienyl (Cp) signals in the course of the reaction of 1 mmol of **2** with TBHP (1 : 20), T = 55 °C (C_6D_6 as the internal standard).

Table 4 Observed ^{19}F NMR shifts and amount of formed insoluble by-products during the reaction with TBHP in compounds **1–4**[a]

Compound	^{19}F NMR shift of prec. [ppm]	Obs. ^{19}F NMR shifts [ppm]	Insol. spec.
1	−62.15	−61.41/−61.74	26%
2	−64.68	−64.49/−64.54/−64.60	20%
3	−63.87	−64.36/−64.50	4%
4	−64.90	−64.78/−64.81/−64.85/−64.88	27%

[a] Pre-catalyst/oxidant ratio = 1 : 20, T = 55 °C, HFB as the internal standard (prec.: precursor, Obs.: observed, insol. spec.: insoluble species).

 This journal is © The Royal Society of Chemistry 2016

Open Access Article. Published on 29 February 2016. Downloaded on 2/9/2026 11:39:55 PM.
This article is licensed under a Creative Commons Attribution-NonCommercial 3.0 Unported Licence.

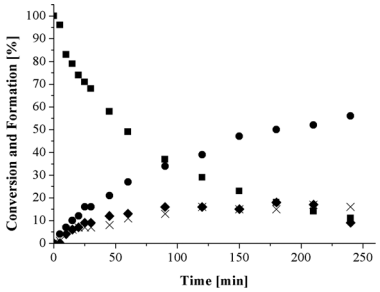

Fig. 9 Kinetic plot of 1 mmol of compound **2** with 10 eq. of *cis*-cyclooctene and 20 eq. of TBHP, T = 55 °C. ■: CF_3 shift of the tricarbonyl precursor. Other symbols: observed CF_3 shifts which form during the reaction with the oxidant. The reaction was followed by ^{19}F NMR spectroscopy in 0.5 ml of C_6D_6 using HFB as the internal standard.

in the ^{19}F NMR spectra is that in the latter case, additional shifts might arise from a changed geometry of the CF_3 group. As reported before in DFT calculations for the $[CpMo(CO)_3CF_3]$ compound, one C–F bond can be elongated and be part of possible interactions with the proton of the oxidant or the molybdenum centre.[21] This change in geometry would lead to the observed additional peaks. Additional DFT calculations with the here reported (more active) fluorinated compounds could help obtain further insights into possible C–F···HOOR or C–F···Mo_{centre} interactions.

Conclusion

Four new CF_3-substituted benzyl molybdenum tricarbonyl complexes have been synthesised, characterised and applied in the oxidation of *cis*-cyclooctene. Differences in reactivity can be largely attributed to different electron densities at the metal, leading to different decarbonylation velocities and epoxidation abilities. This interpretation is supported by ^{95}Mo NMR spectroscopy and DFT calculations. The complexes have also been compared to some benchmark epoxidation catalysts. Addition of a second CF_3 group (in **4**) on the benzyl moiety leads to an increase in activity. It was therefore possible to reach TOFs of $>22\,000$ h^{-1} using HFIP as solvent. The position of the CF_3 group apparently also plays an important role, as compound **1** is more active than **4** – which has one additional CF_3 group – probably due to the location of the CF_3 group which is closer to the molybdenum centre. Moreover, it is possible to recycle the active species for at least 10 runs without loss in activity. It is also possible to oxidise other olefins with **2** and **4**, showing their broader applicability in the oxidation of olefins and, again, the influence of the additional CF_3 group.

Further, ^1H, ^{13}C and ^{19}F NMR kinetic studies made it possible to obtain insights into the nature of the intermediates (dioxo and oxo–peroxo species) during the reaction with TBHP. ^{19}F and ^{13}C NMR kinetics with the addition of a substrate reveal a somewhat modified reaction pathway, favouring one intermediate over the other. As the characterisation of the intermediates is difficult but crucial for further evaluation of a possible mechanism, the findings presented here are helpful in providing a new strategy to obtain one specific intermediate in high yields by adding a substrate. Therefore, future work will focus on the influence of different substrates on the formation of intermediates during the catalytic epoxidation reaction, possibly enabling different intermediates with different substrates.

Experimental section

Material and methods

All experimental synthetic work was carried out using standard Schlenk techniques under argon atmosphere. Catalytic reactions were performed under laboratory atmosphere. Solvents were dried using standard procedures and stored under argon atmosphere over molecular sieves. Commercially available chemicals are used as received, unless stated otherwise. High-resolution NMR spectra were recorded using a Bruker Avance DPX-400 spectrometer (^1H: 400.0 MHz; ^{13}C: 100.6 MHz; ^{19}F: 376.5 MHz). The signals were referenced to the solvent residual signal ($CDCl_3$; ^1H: 7.26 ppm; ^{13}C: 77.16 ppm) or external standards in a capillary (^{95}Mo: $Mo(CO)_6$ in C_6D_6 at −1856 ppm). IR spectra were recorded on a Varian ATR-FTIR instrument. Single crystals suitable for X-ray diffraction were grown by slow diffusion of diethyl ether into saturated solutions of **1–4** in dichloromethane.

Synthesis and characterisation

The organomolybdenum complexes $[CpMo(CO)_3Bz\text{-}o\text{-}CF_3]$ (**1**), $[CpMo(CO)_3Bz\text{-}m\text{-}CF_3]$ (**2**), $[CpMo(CO)_3Bz\text{-}p\text{-}CF_3]$ (**3**) and $[CpMo(CO)_3Bz\text{-}m\text{-}(-CF_3)_2]$ (**4**) as well as literature-known molybdenum and rhenium based complexes $[CpMo(CO)_3Bz]$, $[CpMo(CO)_3BzF_5]$, $[CpMo(CO)_3Cl]$ and methyltrioxorhenium were synthesised according to procedures in the literature.[22,25,38,39]

(1) $[CpMo(CO)_3Bz\text{-}o\text{-}CF_3]$. ^1H-NMR ($CDCl_3$, 298 K, 400 MHz): 7.46–6.99 (m, 4H, Bz), 5.30 (s, 5H, Cp), 2.90 (s, 2H, CH_2Bz); ^{13}C-NMR ($CDCl_3$, 298 K, 101 MHz): 239.81 (CO), 228.72 (CO), 151.93, 131.55, 127.61 (Bz), 125.61 (CF_3), 123.05 (Bz), 93.49 (Cp), 2.96 (CH_2Bz); ^{19}F-NMR ($CDCl_3$, 298 K, 376 MHz): −60.35; ^{95}Mo-NMR (C_6D_6, 298 K, 26 MHz): −1525.24; IR: νCO = 2008.9 cm^{-1} (s), 1986.1 cm^{-1} (vs), 1911.4 cm^{-1} (vs); elemental analysis (calcd.) C: 47.54, H: 2.74, F: 14.10, found: C: 47.86, H: 2.84, F: 14.50 (90% yield, dark yellow powder, m.p. 73 °C).

(2) $[CpMo(CO)_3Bz\text{-}m\text{-}CF_3]$. ^1H-NMR ($CDCl_3$, 298 K, 400 MHz): 7.39–7.22 (m, 4H, Bz), 5.24 (s, 5H, Cp), 2.88 (s, 2H, CH_2Bz); ^{13}C-NMR ($CDCl_3$, 298 K, 101 MHz): 239.19 (CO), 228.21 (CO), 152.37, 130.60, 128.36 (Bz), 123.85 (CF_3), 93.90 (Cp), 3.42 (CH_2Bz); ^{19}F-NMR ($CDCl_3$, 298 K, 376 MHz) −62.78; ^{95}Mo-NMR (C_6D_6, 298 K, 26 MHz): −1558.49; IR: νCO = 2005.9 cm^{-1} (s), 1970.3 cm^{-1} (vs), 1900.0 cm^{-1} (vs); elemental analysis (calcd.) C: 47.54, H: 2.74, F: 14.10, found: C: 47.01, H: 2.83, F: 14.40 (88% yield, yellow powder, m.p. 107 °C).

(3) $[CpMo(CO)_3Bz\text{-}p\text{-}CF_3]$. ^1H-NMR ($CDCl_3$, 298 K, 400 MHz): 7.40 (m, 2H, Bz), 7.25 (m, 2H, Bz), 5.23 (s, 5H, Cp),

Open Access Article. Published on 29 February 2016. Downloaded on 2/9/2026 11:39:55 PM.
This article is licensed under a Creative Commons Attribution-NonCommercial 3.0 Unported Licence.

2.85 (s, 2H, CH_2Bz); ^{13}C-NMR ($CDCl_3$, 298 K, 101 MHz): 239.15 (CO), 228.25 (CO), 156.07, 127.42 (Bz), 124.93 (CF_3), 93.95 (Cp), 3.43 (CH_2Bz); ^{19}F-NMR ($CDCl_3$, 298 K, 376 MHz) −61.94; ^{95}Mo-NMR (C_6D_6, 298 K, 26 MHz): −1562.52; IR: νCO = 2008.1 cm^{-1} (s), 1972.5 cm^{-1} (vs), 1902.7 cm^{-1} (vs); elemental analysis (calcd.) C: 43.24, H: 2.13, F: 24.14, found: C: 43.40, H: 2.23, F: 24.51 (87% yield, yellow powder, m.p. 93 °C).

(4) [$CpMo(CO)_3Bz$-*m*-$(-CF_3)_2$]. ^{1}H-NMR ($CDCl_3$, 298 K, 400 MHz): 7.54 (s, 2H, Bz), 7.46 (s, 1H, Bz), 5.29 (s, 5H, Cp), 2.86 (s, 2H, CH_2Bz); ^{13}C-NMR ($CDCl_3$, 298 K, 101 MHz): 238.33 (CO), 228.19 (CO), 153.99, 131.12, 126.90, 125.08, 122.38 (Bz), 117.08 (CF_3), 93.74 (Cp), 2,22 (CH_2Bz); ^{19}F-NMR ($CDCl_3$, 298 K, 376 MHz) −63.07; ^{95}Mo-NMR (C_6D_6, 298 K, 26 MHz): −1537.10; IR: νCO = 2014.8 cm^{-1} (s), 1950.6 cm^{-1} (vs), 1916.3 cm^{-1} (vs); elemental analysis (calcd.) C: 47.54, H: 2.74, F: 14.10, found: C: 47.15, H: 2.88, F: 14.46 (85% yield, yellow powder, m.p. 101 °C).

(I) Insoluble species. Elemental analysis (found): C: 19.20, H: 3.05, F: 3.44, Mo: 33.13 O: not determined; *m*/*z* 241.1 (FAB), 227.2 (base).

Recycling experiments

After the catalytic reaction in 2.5 ml of the IL (1,2-dimethyl-3-octyl imidazoliumbis(trifluoromethylsulfonyl)imide), the upper phase was removed from the reaction vessel by addition of 5 mL of *n*-hexane after cooling to room temperature. The lighter phase was removed using a cannula. The samples were treated with MnO_2 to remove water and eliminate excess peroxide. Afterwards, the sample was diluted with C_6D_6 and the resulting slurry was filtered and transferred to an NMR tube. Additionally, oil pump vacuum for 4 h at 55 °C allowed the removal of ^{t}BuOH from the remaining RTIL phase before further *cis*-cyclooctene and TBHP were added.

Kinetic experiments

Kinetic experiments were performed in an NMR tube equipped with a respective pre-catalyst (0.1 mmol), solvent (0.5 ml of $CDCl_3$ or C_6D_6), an internal standard (0.1 mmol of mesitylene or hexafluorobenzene) and (if needed) *cis*-cyclooctene (1 mmol). The reaction started with the addition of TBHP (5.5 M in *n*-decane; 2 mmol) at an applied temperature. The course of the reaction was monitored by ^{1}H, ^{13}C, ^{19}F or ^{95}Mo NMR spectroscopy.

X-ray single crystal structure determination

Single crystals suitable for X-ray diffraction were grown by slow diffusion of diethyl ether into a saturated solution of **1–4** in dichloromethane. CCDC numbers for complexes **1–4** are located in Table S1 (ESI†).

Computational details

All calculations have been performed using Gaussian03.[40] The level of theory contains the hybrid DFT functional B3LYP[41,42] and the double zeta 6-31 + G**[43] basis set for all the atoms excluding Mo, and the Stuttgart 1997 ECP for molybdenum.[44] All the obtained geometries have been identified using the numbers of negative frequencies as minima (NI_{mag} = 0). Free energy differences have been calculated for the gas phase at 298.15 K and 1.0 atm.

Acknowledgements

R. M. R. and M. K. thank the TUM Graduate School for financial support, Dr. Markus Drees for helpful discussions concerning the DFT calculations and Maria Weindl as well as Jürgen Kudermann for NMR spectroscopy.

Notes and references

1 S. Huber, M. Cokoja and F. E. Kühn, *J. Organomet. Chem.*, 2014, **751**, 25–32.
2 S. A. Hauser, M. Cokoja and F. E. Kühn, *Catal. Sci. Technol.*, 2013, **3**, 552–561.
3 F. Cavani and J. H. Teles, *ChemSusChem*, 2009, **2**, 508–534.
4 T. A. Nijhuis, M. Makkee, J. A. Moulijn and B. M. Weckhuysen, *Ind. Eng. Chem. Res.*, 2006, **45**, 3447–3459.
5 J. Kollar, Halcon International, Inc., *US Pat.* 3351635, 1967.
6 N. Grover and F. E. Kühn, *Curr. Org. Chem.*, 2012, **16**, 16–32.
7 K. R. Jain and F. E. Kühn, *Dalton Trans.*, 2008, 2221–2227.
8 F. E. Kühn, A. M. Santos and M. Abrantes, *Chem. Rev.*, 2006, **106**, 2455–2475.
9 C. Freund, M. Abrantes and F. E. Kühn, *J. Organomet. Chem.*, 2006, **691**, 3718–3729.
10 S. M. Bruno, J. A. Fernandes, L. S. Martins, I. S. Gonçalves, M. Pillinger, P. Ribeiro-Claro, J. Rocha and A. A. Valente, *Catal. Today*, 2006, **114**, 263–271.
11 A. A. Valente, J. D. Seixas, I. S. Gonçalves, M. Abrantes, M. Pillinger and C. C. Romão, *Catal. Lett.*, 2005, **101**, 127–130.
12 A. Schmidt, N. Grover, T. K. Zimmermann, L. Graser, M. Cokoja, A. Pöthig and F. E. Kühn, *J. Catal.*, 2014, **319**, 119–126.
13 D. Betz, A. Raith, M. Cokoja and F. E. Kühn, *ChemSusChem*, 2010, **3**, 559–562.
14 C. C. Romão, F. E. Kühn and W. A. Herrmann, *Chem. Rev.*, 1997, **97**, 3197–3246.
15 B. R. Goldsmith, T. Hwang, S. Seritan, B. Peters and S. L. Scott, *J. Am. Chem. Soc.*, 2015, **137**, 9604–9616.
16 P. Chaumette, H. Mimoun, L. Saussine, J. Fischer and A. Mitschler, *J. Organomet. Chem.*, 1983, **250**, 291–310.
17 H. Mimoun, I. S. D. Roch and L. Sajus, *Tetrahedron*, 1970, **26**, 37–50.
18 K. B. Sharpless, D. R. Williams and J. M. Townsend, *J. Am. Chem. Soc.*, 1972, **94**, 295–296.
19 W. R. Thiel and T. Priermeier, *Angew. Chem., Int. Ed. Engl.*, 1995, **34**, 1737–1738.
20 N. Grover, M. Drees and F. E. Kühn, *J. Catal.*, 2015, **329**, 269–285.
21 M. Drees, S. A. Hauser, M. Cokoja and F. E. Kühn, *J. Organomet. Chem.*, 2013, **748**, 36–45.
22 M. Abrantes, A. M. Santos, J. Mink, F. E. Kühn and C. C. Romao, *Organometallics*, 2003, **22**, 2112–2118.

 This journal is © The Royal Society of Chemistry 2016

Open Access Article. Published on 29 February 2016. Downloaded on 2/9/2026 11:39:55 PM.
This article is licensed under a Creative Commons Attribution-NonCommercial 3.0 Unported Licence.

23 A. Comas-Vives, A. Lledos and R. Poli, *Chem. – Eur. J.*, 2010, **16**, 2147–2158.
24 P. J. Costa, M. J. Calhorda and F. E. Kühn, *Organometallics*, 2010, **29**, 303–311.
25 S. A. Hauser, M. Cokoja, M. Drees and F. E. Kühn, *J. Mol. Catal. A: Chem.*, 2012, **363–364**, 237–244.
26 S. A. Hauser, R. M. Reich, J. Mink, A. Pöthig, M. Cokoja and F. E. Kühn, *Catal. Sci. Technol.*, 2015, **5**, 2282–2289.
27 L. Graser, R. M. Reich, M. Cokoja, A. Pöthig and F. E. Kühn, *Catal. Sci. Technol.*, 2015, **10**, 4772–4777.
28 D. J. Parker and M. H. B. Stiddard, *J. Chem. Soc. A*, 1970, 480–490.
29 D. J. Parker, *J. Chem. Soc. A*, 1970, 1382–1386.
30 R. B. King and L. W. Houk, *Can. J. Chem.*, 1969, **47**, 2959–2964.
31 R. B. King and M. B. Bisnette, *J. Organomet. Chem.*, 1964, **2**, 15–37.
32 M. Minelli, J. H. Enemark, R. T. C. Brownlee, M. J. O'connor and A. G. Wedd, *Coord. Chem. Rev.*, 1985, **68**, 169–278.
33 W. A. Herrmann and F. E. Kühn, *Acc. Chem. Res.*, 1997, **30**, 169–180.
34 W. A. Herrmann, F. E. Kühn, R. W. Fischer, W. R. Thiel and C. C. Romao, *Inorg. Chem.*, 1992, **31**, 4431–4432.
35 W. A. Herrmann, J. G. Kuchler, J. K. Felixberger, E. Herdtweck and W. Wagner, *Angew. Chem., Int. Ed. Engl.*, 1988, **27**, 394–396.
36 N. Grover, A. Pöthig and F. E. Kühn, *Catal. Sci. Technol.*, 2014, **4**, 4219–4231.
37 P. Altmann, M. Cokoja and F. E. Kühn, *Eur. J. Inorg. Chem.*, 2012, 3235–3239.
38 J. K. M. Mitterpleininger, N. Szesni, S. Sturm, R. W. Fischer and F. E. Kühn, *Eur. J. Inorg. Chem.*, 2008, 3929–3934.
39 R. B. King and A. Fronzaglia, *J. Am. Chem. Soc.*, 1966, **88**, 709–712.
40 M. J. Frisch, H. B. Schlegel, G. E. Scuseria, M. A. Robb, J. R. Cheeseman, J. A. Montgomery Jr, T. Vreven, K. N. Kudin, J. C. Burant, J. M. Millam, S. S. Iyengar, J. Tomasi, V. Barone, B. Mennucci, M. Cossi, G. Scalmani, N. Rega, G. A. Petersson, H. Nakatsuji, M. Hada, M. Ehara, K. Toyota, R. Fukuda, J. Hasegawa, M. Ishida, T. Nakajima, Y. Honda, O. Kitao, H. Nakai, M. Klene, X. Li, J. E. Knox, H. P. Hratchian, J. B. Cross, V. Bakken, C. Adamo, J. Jaramillo, R. Gomperts, R. E. Stratmann, O. Yazyev, A. J. Austin, R. Cammi, C. Pomelli, J. W. Ochterski, P. Y. Ayala, K. Morokuma, G. A. Voth, P. Salvador, J. J. Dannenberg, V. G. Zakrzewski, S. Dapprich, A. D. Daniels, M. C. Strain, O. Farkas, D. K. Malick, A. D. Rabuck, K. Raghavachari, J. B. Foresman, J. V. Ortiz, Q. Cui, A. G. Baboul, S. Clifford, J. Cioslowski, B. B. Stefanov, G. Liu, A. Liashenko, P. Piskorz, I. Komaromi, R. L. Martin, D. J. Fox, T. Keith, M. A. Al-Laham, C. Y. Peng, A. Nanayakkara, M. Challacombe, P. M. W. Gill, B. Johnson, W. Chen, M. W. Wong, C. Gonzalez and J. A. Pople, *Gaussian03*, Gaussian, Inc., Wallingford, CT, 2004.
41 A. D. Becke, *J. Chem. Phys.*, 1993, **98**, 5648–5652.
42 Y. W. C. Lee and R. G. Parr, *Phys. Rev. B: Condens. Matter*, 1988, **37**, 785–789.
43 R. D. J. Hehre and J. A. Pople, *J. Chem. Phys.*, 1972, **56**, 2257–2261.
44 A. Bergner, M. Dolg, W. Küchle, H. Stoll and H. Preuß, *Mol. Phys.*, 1993, **80**, 1431–1441.